Advance Publication

Experimental Animals

Received: 2022.7.28

Accepted: 2022.11.26

J-STAGE Advance Published Date: 2022.12.5

Loss of AKAP12 aggravates rheumatoid arthritis-like symptoms and cardiac damage in collagen-induced arthritis mice

Running Head: AKAP12 loss aggravates rheumatoid arthritis

YANHUI NI[1, *]; JINGJING CAO[2]; JING YUAN[1]; XIAORAN NING[2]

[1]Department of Cardiology, Hebei General Hospital, Shijiazhuang 050051, Hebei, China.

[2]Department of Rheumatology and Immunology, Hebei General Hospital, Shijiazhuang 050051, Hebei, China.

[*]Correspondence: Yanhui Ni, Department of Cardiology, Hebei General Hospital, 348 Heping West Road, Shijiazhuang 050051, Hebei, China.

E-mail: niyanhui1983@163.com

Phone: +86-311-85988265

Abstract

A-kinase anchoring protein 12 (AKAP12) has been identified as an anti-inflammatory and anti-fibrotic regulator in chronic inflammation and cardiovascular disease. However, the potential of AKAP12 in autoimmune disorders, rheumatoid arthritis (RA) and associated cardiac complications remains elusive. Here, a murine model of collagen-induced arthritis (CIA) was successfully induced, followed by adenovirus-mediated AKAP12 short hairpin RNA (shRNA) treatment. AKAP12 silenced mice displayed elevated clinical arthritis scores and significant ankle joint swelling. AKAP12 loss in CIA mice increased inflammatory cell infiltration and cartilage erosion, increased the levels of anti-IIC IgG and inflammatory cytokines IL-1β, IL-6, TNF-α in serum, and upregulated the expression of cartilage-degrading enzymes MMP-1, MMP-3, MMP-13 in synovium, but reduced IL-10. The number of M1 macrophages and the expression of the markers (CCR7, IL-6, TNF-α and iNOS) was enhanced in synovial tissues, while M2 polarized macrophages and the makers (IL-10 and arginase-1) were reduced in response to AKAP12 loss. Moreover, low expression of AKAP12 was detected in the hearts of CIA mice. Loss of AKAP12 results in increased cardiac inflammation and fibrosis. This work suggests that AKAP12 loss aggravates joint inflammation likely through the promotion of M1 macrophage polarization and exacerbates inflammation-caused cardiac fibrosis.

Keywords: rheumatoid arthritis, AKAP12, inflammation, macrophage polarization, heart

Introduction

Rheumatoid arthritis (RA) is a chronic autoimmune polyarticular disorder that affects about 1% population in the world [1]. Clinically, it is mainly characterized by destructive inflammation in synovial joints, leading to cartilage degradation and eventual disability [2]. Pathogenic alterations in synovium are predominantly caused by the increase and activation of synovial macrophages, with the production of inflammatory cytokines, matrix metalloproteinases (MMPs) and cartilage-degrading enzymes [3]. At present, the treatment of this disease includes non-steroidal anti-inflammatory drugs, glucocorticoid and disease modifying anti-rheumatic drugs (DMARD) therapy, yet the effect is not satisfactory [4]. RA is also a complex multisystem disease, and RA inflammation is associated with the occurrence of extra-articular complications, including early cardiovascular death [5], which increased the difficulty in the treatment of RA. Therefore, novel treatment strategies for preventing RA and its complications are urgently required.

A-kinase anchoring protein 12 (AKAP12), a scaffolding protein, anchors protein kinase A (PKA) and protein kinase C (PKC) to the plasma membrane to regulate cytoskeletal structure, cell migration and attachment [6, 7]. The anti-migration and invasion actions of AKAP12 have been widely described in a bunch of cancers [6, 8], but the functionality of AKAP12 in RA is still undefined. AKAP12 has been implicated in the regulation of inflammatory reaction, and low AKAP12 expression is found in lung tissues of patients with chronic pneumonia [9]. AKAP12 knockdown in fibrotic scars results in excessive inflammation [10], and it accelerates macrophage

polarization towards an anti-inflammatory M2 phenotype during inflammation recovery [11]. Moreover, several studies have indicated the function of AKAP12 in cardiovascular diseases [12]. AKAP12 depletion promotes lipopolysaccharide-triggered inflammatory cytokine changes and vascular endothelial dysfunction [13], and leads to inflammation and cell apoptosis in angiotensin II-caused cardiac damage [14]. AKAP12 expression is obviously downregulated in RA synovial tissues [15]. We hypothesize that AKAP12 may be a valuable target for the treatment of RA and associated myocardial damage.

In current work, collagen-induced arthritis (CIA), a murine model of RA, was established and we treated CIA mice with adenovirus expressing AKAP12 short hairpin RNA (shRNA) to explore the effect of AKAP12 on joint inflammation and cardiac complications. Our study provides a theoretical basis for the treatment of RA and related heart diseases by targeting AKAP12.

Materials and methods

Materials

Bovine type II collagen (CII) was purchased from Source Leaf Biological Technology Co., Ltd. (Shanghai, China). Hemotoxylin and SYBR Green were from Solarbio Life Sciences (Beijing, China), and Eosin was obtained from Sangon Biotechnology (Shanghai, China). AKAP12, MMP-1 and CD206 antibodies were purchased from Proteintech, MMP-3 and MMP-13 antibodies were from Affinity, and Goat anti-rabbit IgG was from ThermoFisher (China). CD68 antibody was obtained from Abcam (UK)

and anti-CCR7 was from ABclonal (China). 3,3'-diaminobenzidine (DAB) chromogenic solution was obtained from Fuzhou Maixin Biotech (China). The primers used were synthesized by GenScript (Nanjing, China). TRIpure reagent was bought from BioTeke (Beijing, China). Electrochemiluminescence (ECL) reagent was provided by Beyotime Biotechnology (Shanghai, China). Anti-collagen type II (CII) antibody enzyme-linked immunosorbent assay (ELISA) kit was from FineTest (Wuhan, China). The kits for detecting interleukin (IL)-1β, IL-6, tumor necrosis factor (TNF)-α and IL-10 levels were acquired from MultiSciences (Hangzhou, China).

Experimental animals and treatment

Male DBA/1 mice (6-8 weeks old) obtained were kept in a suitable environment with food and water freely available. The animal experiments were conducted with the approval of the Experimental Animal Ethics Committee at the Hebei General Hospital (approval no. 2021-71). The CIA mouse model was established according to previous research [16]. CII (2 mg/mL) emulsified with equal amounts (1:1, v/v) of Freund's complete adjuvant (primary immunization) or Freund's incomplete adjuvant (secondary immunization) was prepared. On day 0, the mice were immunized by subcutaneous injection of 0.1 mL emulsion at the base of the tail. A booster immunization was performed on day 21. The mice were boosted subcutaneously with CII emulsified with Freund's incomplete adjuvant (0.1 mL).

The adenovirus-based shRNA vectors were synthesized by General Biosystems (Anhui, China) and constructed into the pShuttle-CMV vector (Hunan Fenghui

Biotechnology Co., Ltd., China). The sequence of AKAP12 shRNA was GCTTCAAGAAGGTATTTAAAT, which was synthesized by General Biosystems (Anhui, China).

Recombinant adenoviruses carrying AKAP12 shRNA (shAKAP12) or negative control shRNA (shNC) were prepared. Then, the adenoviruses (Ad-shAKAP12 or Ad-shNC) were administrated once a week via tail vein injection at a dose of 10^8 PFU/mouse. The clinical arthritis score and hind paw thickness were monitored at 2-day intervals starting in day 23 of CIA modeling. The scoring method was based on a previous study [16]. In detail, each paw was assessed and scored individually, with a score of 4 representing the most severe degree of inflammation. The sum of the scores for all 4 climbs was calculated as an arthritis index for each animal, with a maximum index score of 16. Besides, the thickness (mm) of the hind paw was measured using a caliper. On day 32, all mice were euthanized by intraperitoneal injection of sodium pentobarbital (200 mg/kg) [17]. Blood samples were collected from the retro-orbital venous plexus of mice. The ankle joints, synovium, synovial fluid and hearts were then harvested.

Histopathological examination

Synovial and heart tissues were fixed in 4% paraformaldehyde overnight, followed by paraffin-embedding for histopathological analysis. Samples were sliced into 5 μm thickness, and stained with hemotoxylin and eosin (H&E) or safranin *O* and fast green. The stained sections were then observed and photographed under a light microscope

(Olympus, Tokyo, Japan). Synovial inflammation and cartilage erosion were assessed and scored [18, 19]. The synovitis scoring was based on the following criteria: no synovitis (0-1), low-grade synovitis (2-4), high-grade synovitis (5-9). Cartilage erosion was determined using the Osteoarthritis Research Society International (OARSI) scoring system. The scoring standards were defined as follows: intact surface and cartilage morphology (grade 0), intact surface (grade 1), discontinuous surface (grade 2), vertical fissures (grade 3), erosion (grade 4), denudation (grade 5), and deformation (grade 6). Myocardial damage was determined and scored in accordance with the percentage of positive staining area, and the specific criteria were as follows [20]: minimal, < 25% (1); moderate, 25–50% (2); significant, 50–75% (3); severe, > 75% (4). The sum of three variables was used to represent the cardiac damage score (0-12). For evaluation of fibrosis, the heart tissue sections were stained with Masson trichrome reagent in accordance with the instruction of manufacturer. The quantitative analysis of Masson-positive staining area was done using the image analysis software (Image-Pro Plus6.0), and the percentage of positive-staining area was calculated (area of positive staining / area of tissue × 100).

Immunohistochemistry

Paraffin-embedded synovial samples (5 μm thick) were rehydrated and antigen-retrieved, and primary antibody (AKAP12 antibody, 1:200) was added and incubated overnight at 4℃. Incubation of horseradish peroxidase (HRP)-labeled secondary antibody (1:500) was then performed for 1 h. After staining with DBA and

hematoxylin, the slices were imaged by a microscope at 400× magnification.

Quantitative PCR

Primers utilized for quantitative PCR were shown in Table 1. Total mRNAs were obtained from synovial tissues, synovial fluid and hearts using TRIpure as recommended by the manufacturer. Reverse transcription was carried out using the BeyoRT II M-MLV reverse transcriptase (Beyotime, Shanghai, China). Quantification of mRNA was based on SYBR green PCR system. Mouse β-actin served as the amplification control.

Western blot

Mouse synovial and heart tissue samples were lysed and centrifuged, and the proteins from the supernatant were run on 10% SDS-polyacrylamide gel electrophoresis (PAGE). Proteins were then transferred onto the PVDF membranes, and the membranes were blocked with 5% skimmed milk powder for 1 hour. They were probed with primary antibody against AKAP12 (1:1000), MMP-1 (1:500), MMP-3 (1:1000) or MMP-13 (1:1000), and later incubated with HRP-conjugated goat anti-rabbit secondary antibody (1:10000). Forty minutes later, the blots were visualized using ECL. Optical density value was obtained using Tanon Image Analyzer (Shanghai, China).

ELISA

Mouse serum anti-CII antibody and inflammatory cytokines IL-1β, IL-6, TNF-α and

IL-10 levels were determined by ELISA according to the standard methods provided by the manufacturers.

Immunofluoresence double staining

Sections (5 μm) prepared were incubated with first antibodies anti-CD68 (1:50), anti-CD206 and anti-CCR7 (1:100) at 4℃ overnight. The goat anti-mouse (FITC) or anti-rabbit (Cy3) secondary antibody (1:200) was added and incubated for 1.5 h in the dark. The nucleus was visualized using 4’,6-diamidino-2-phenylindole (DAPI, blue). The sections were finally mounted and photographed using fluorescence microscopy (Olympus, Tokyo, Japan).

Statistical analysis

The values were shown as the mean ± standard deviation (SD) from at least six independent experiments. Data analysis was done using the GraphPad Prism 8.0, GraphPad Software. Statistical comparisons between control and model were based on the unpaired Student’s *t* test, and differences among multiple groups were assessed using the one-way analysis of variance (ANOVA) followed by Tukey’s multiple comparisons test. $P < 0.05$ was pre-specified as statistically significant.

Results

AKAP12 expression in CIA mice

CIA is a widely used animal model of RA, and the experimental design of this study

was depicted in Fig. 1A. Compared with the control group, CIA mice displayed obvious increases in arthritis scores and hind paw thickness from the 23th day to the 32nd day (Fig. 1B). Fig. 1C showed the representative photographs of the injured paws of mice at day 32, and obvious swelling and redness were observed in the hind paws of CIA mice. These data suggest that RA model in mice were established successfully. We then examined the expression of AKAP12 by quantitative PCR, western blot and immunohistochemistry assays. Relative mRNA level of AKAP12 was significantly downregulated in synovial tissues and fluid of CIA mice (Fig. 1D). This finding was further supported by immunohistochemistry and western blot data (Fig. 1E and F).

Loss of AKAP12 aggravates CIA development in mice

To evaluate AKAP12's function in RA, CIA mice were treated with adenovirus expressing AKAP12 shRNA. Compared with the control mice, AKAP12 shRNA caused increased clinical scores and severe paw swelling in mice (Fig. 2A and B), demonstrating that AKAP12 shRNA-treated mice develop severe CIA. AKAP12 expression in synovium was silenced by adenovirus transduction of AKAP12 shRNA, as demonstrated by quantitative PCR and western blot analysis (Fig. 2C). Loss of AKAP12 increased serum anti-IIC IgG level (Fig. 2D). Histopathological examination found that CIA mice exhibited inflammatory cell infiltration in synovial tissues, cartilage destruction and bone erosion in ankle joints, which was enhanced by AKAP12 loss (Fig. 3A and B). Thus, AKAP12 loss aggravates CIA-caused joint damage in mice.

AKAP12 loss alters the inflammatory properties in CIA mice

Proinflammatory cytokines are critical regulators participating in joint inflammation and cartilage degradation [21]. Levels of serum inflammatory factors were measured by ELISA. CIA mice displayed significant elevation in IL-1β, IL-6, TNF-α and IL-10. AKAP12 shRNA-treated mice showed further increases in IL-1β, IL-6 and TNF-α, but a decrease in IL-10 (Fig. 4A). Besides, the relative expression of MMP-1, MMP-3 and MMP-13 was upregulated in synovial tissues of CIA mice, which further enhanced by AKAP12 loss (Fig. 4B). All these data suggest that loss of AKAP12 was capable of enhancing inflammatory response in RA.

AKAP12 loss affects the phenotypic changes of macrophages in CIA mice

Macrophages exhibit two main classifications, “proinflammatory” M1 and anti-inflammatory “M2” [22]. Immunofluorescence double staining for CD68 (M0 macrophage marker) and CCR7 (M1 macrophage marker) was performed in the synovial tissues. A large area of CCR7 staining was observed in CIA mice, and AKAP12 loss enhanced it (Fig. 5A). IL-6, TNF-α and iNOS are the major products of M1 macrophages, and quantitative PCR results verified that loss of AKAP12 significantly elevated CIA-induced increases in IL-6, TNF-α and iNOS mRNA levels (Fig. 5B). Besides, a small area of CD206 (M2 marker) staining was found following AKAP12 shRNA treatment (Fig. 6A). Loss of AKAP12 could lower the mRNA levels of IL-10 and arginase-1, two recognized markers of M2 macrophages (Fig. 6B). These findings indicate that AKAP12 loss is able to drive the phenotypic switch from M2 to

M1 macrophages.

Loss of AKAP12 aggravates myocardial damage induced by CIA

RA patients are at high risk for heart disease [23]. Quantitative PCR and western blot analysis confirmed that the mRNA and protein expression levels of AKAP12 were downregulated remarkably in the hearts of CIA model mice, which were decreased by AKAP12 shRNA (Fig. 7A). H&E staining of the hearts was shown in Fig. 7B. The control mice displayed normal myocardial structure. AKAP12 loss worsened CIA-caused inflammatory cell infiltration and misaligned myofibrillar structure. Masson staining in Fig. 7C demonstrated that AKAP12 shRNA-treated mice had a higher proportion of fibrosis compared to the CIA group, as manifested by strong blue collagen staining. These results indicate that AKAP12 loss may exacerbate CIA-induced cardiac failure.

Discussion

RA is a common inflammatory arthritis, primarily affecting synovium and joint cartilage. In our study, we investigated the potential of AKAP12 in RA progression using a CIA murine model. AKAP12 loss was found to aggravate joint swelling, inflammation and bone destruction possibly via the promotion of M1 macrophage polarization. It also damaged CIA-induced heart tissues demonstrated by enhanced cardiac fibrosis. Thus, AKAP12 may act as a potential target for the therapy of RA and its cardiac complications.

Type II collagen can induce RA-like symptoms in mice and stimulate

autoimmune and inflammatory responses [24, 25]. DBA/1 mice have been reported to have high sensitivity in CIA model [26]. Here, CIA mice displayed visible joint swelling and arthritis, similar to the features of RA.

Joint damage in RA is associated with cartilage degradation and extracellular matrix destruction [27, 28]. We first confirmed that AKAP12 was low-expressed in synovial tissues and synovial fluid of CIA mice, and its loss can result in the erosion of cartilages in the synovium, indicating the importance of AKAP12 in RA. The extracellular matrix, including collagen, is the main component of articular cartilage, which can maintain the structural integrity of cartilage and homeostasis of the extracellular environment [28]. MMP family members including MMP-1, MMP-3 and MMP-13 are reported to serve as collagenases mediating the degradation of extracellular matrix [28, 29]. AKAP12 deletion elevated MMP expression in RA synovium, thereby enhancing CIA-induced matrix degradation. Besides, the production of MMPs is stimulated by inflammatory cytokines such as TNF-α and IL-1β [28]. Chronic inflammation in RA is attenuated by the decrease in proinflammatory factors IL-1β, IL-6, TNF-α and the increase in anti-inflammatory IL-10 [30, 31]. Li et al. reported the proinflammatory function of AKAP12 deletion in damaged mice [14]. Our study further confirmed that AKAP12 loss had a proinflammatory role in RA. These data support the notion that loss of AKAP12 aggravates CIA-caused joint damage through promoting synovial inflammation and MMPs-mediated cartilage degradation.

Macrophages are broadly distributed immune cells, and their increase in

inflamed joints is recognized as an early marker of active RA [32]. Activated macrophages drive the progression of RA by producing proinflammatory cytokines and MMPs [33, 34]. RA inflammation and tissue destruction are mediated by the polarization of synovial macrophages (proinflammatory M1 and anti-inflammatory M2) [32, 35]. Yang et al. found that AKAP12 knockdown lowers the proportion of M2 macrophages by declining the expression of M2 markers CD206 and arginase 1 [11]. CCR7 is a hallmark for macrophage M1 phenotype [36, 37]. CCR7 knockout prevents CIA progression in mice [38]. Prevention of M1 macrophage polarization may be a potential therapeutic approach for RA. Consistent with previous studies, AKAP12 loss in synovium skewed macrophage polarization toward the M1 phenotype. Increased proportion of M1 macrophages was observed in CIA mice. Activated M1 macrophages can produce a variety of proinflammatory cytokines including IL-6, TNF-α and iNOS, aggravating joint inflammation [39]. The proinflammatory function of AKAP12 loss was found in the synovium of CIA mice, as manifested by increased expression of proinflammatory factors and reduced anti-inflammatory mediators. These results suggest that AKAP12 loss-mediated joint damage in RA may be modulated by the polarization of M1 macrophages. The joint synovium contains a variety of cells, including the fibroblast-like synoviocytes (FLS) [40], synovial macrophages [41], and chondrocytes [42]. A limitation of our study is the lack of *in vitro* analysis, and whether AKAP12 functions in CIA-related cell types will be investigated in the future.

Patients with RA have a high incidence of cardiovascular complications [43].

Joint inflammation caused by CIA promotes the progression of myocardial fibrosis, contributing to heart failure development [44]. CIA mice exhibited obvious inflammatory cell infiltration and severe fibrosis in the hearts, which is in line with the finding of Wang et al. [45]. AKAP12 deletion has been reported to promote inflammatory response and cardiac fibrosis [14]. In this study, AKAP12 expression was downregulated in the hearts of CIA mice, and the profibrotic role of AKAP12 loss was verified. Moreover, the accumulation of inflammatory cytokines in rheumatoid synovium can drive a series of maladaptive processes in the myocardium, thereby causing myocardial dysfunction [46]. The precise mechanisms underpinning the relationship between RA and cardiovascular diseases are not well established. Our experiments reveal that loss of AKAP12 may be detrimental to the attenuation of RA and associated cardiac failure. Cardiovascular event is one of the common complications of RA patients. Synovitis can also stimulate other systemic disorders such as osteoporosis and fracture, metabolic syndrome and pulmonary disorder [3]. Therefore, additional research is required.

In conclusion, the current study uncovered that AKAP12 loss aggravated joint damage, synovial inflammation and cardiac complications in CIA mice, providing a potential therapeutic target for RA and related cardiac complications.

Funding

Not applicable

Authors' Contributions

YN and JC designed the study and performed the experiments. JY and XN analyzed the data. YN drafted and revised the manuscript. All authors reviewed and approved the submission.

Ethics Approval and Consent to Participate

All animal experiments were performed with the approval of the Experimental Animal Ethics Committee at the Hebei General Hospital.

Conflict of Interest

The authors claim no conflict of interest to disclose.

Data Availability Statement

All data generated or analyzed in our work are included in this paper.

Acknowledgments

Not applicable

References

1. Smolen J S, Aletaha D, McInnes I B. Rheumatoid arthritis. *Lancet*. 2016; 388 (10055): 2023-2038.

2. Schett G, Gravallese E. Bone erosion in rheumatoid arthritis: mechanisms, diagnosis and treatment. *Nat Rev Rheumatol*. 2012; 8 (11): 656-64.

3. McInnes I B, Schett G. The pathogenesis of rheumatoid arthritis. *N Engl J Med*. 2011; 365 (23): 2205-19.

4. Burmester G R, Pope J E. Novel treatment strategies in rheumatoid arthritis. *Lancet*. 2017; 389 (10086): 2338-2348.

5. Turiel M, Sitia S, Atzeni F, Tomasoni L, Gianturco L, Giuffrida M, et al. The heart in rheumatoid arthritis. *Autoimmun Rev*. 2010; 9 (6): 414-8.

6. Wu X, Wu T, Li K, Li Y, Hu T T, Wang W F, et al. The Mechanism and Influence of AKAP12 in Different Cancers. *Biomed Environ Sci*. 2018; 31 (12): 927-932.

7. Wong W, Scott J D. AKAP signalling complexes: focal points in space and time. *Nat Rev Mol Cell Biol*. 2004; 5 (12): 959-70.

8. Su B, Bu Y, Engelberg D, Gelman I H. SSeCKS/Gravin/AKAP12 inhibits cancer cell invasiveness and chemotaxis by suppressing a protein kinase C- Raf/MEK/ERK pathway. *J Biol Chem*. 2010; 285 (7): 4578-86.

9. Poppinga W J, Heijink I H, Holtzer L J, Skroblin P, Klussmann E, Halayko A J, et al. A-kinase-anchoring proteins coordinate inflammatory responses to cigarette smoke in airway smooth muscle. *Am J Physiol Lung Cell Mol Physiol*. 2015; 308 (8):

L766-75.

10. Cha J H, Wee H J, Seo J H, Ahn B J, Park J H, Yang J M, et al. AKAP12 mediates barrier functions of fibrotic scars during CNS repair. *PLoS One*. 2014; 9 (4): e94695.

11. Yang J M, Lee H S, Seo J H, Park J H, Gelman I H, Lo E H, et al. Structural environment built by AKAP12+ colon mesenchymal cells drives M2 macrophages during inflammation recovery. *Sci Rep*. 2017; 7: 42723.

12. Qasim H, McConnell B K. AKAP12 Signaling Complex: Impacts of Compartmentalizing cAMP-Dependent Signaling Pathways in the Heart and Various Signaling Systems. *J Am Heart Assoc*. 2020; 9 (13): e016615.

13. Li Z, Hu J, Guo J, Fan L, Wang S, Dou N, et al. SSeCKS/Gravin/AKAP12 Inhibits PKCζ-Mediated Reduction of ERK5 Transactivation to Prevent Endotoxin-Induced Vascular dysfunction. *Cardiovasc Toxicol*. 2019; 19 (4): 372-381.

14. Li Y, Yu Q H, Chu Y, Wu W M, Song J X, Zhu X B, et al. Blockage of AKAP12 accelerates angiotensin II (Ang II)-induced cardiac injury in mice by regulating the transforming growth factor β1 (TGF-β1) pathway. *Biochem Biophys Res Commun*. 2018; 499 (2): 128-135.

15. Chen Y J, Chang W A, Hsu Y L, Chen C H, Kuo P L. Deduction of Novel Genes Potentially Involved in Osteoblasts of Rheumatoid Arthritis Using Next-Generation Sequencing and Bioinformatic Approaches. *Int J Mol Sci*. 2017; 18 (11).

16. Brand D D, Latham K A, Rosloniec E F. Collagen-induced arthritis. *Nat Protoc*. 2007; 2 (5): 1269-75.

17. Wu C T, Haggerty D, Kemere C, Ji D. Hippocampal awake replay in fear memory

363 retrieval. *Nat Neurosci*. 2017; 20 (4): 571-580.
364 18. Krenn V, Morawietz L, Burmester G R, Kinne R W, Mueller-Ladner U, Muller B,
365 et al. Synovitis score: discrimination between chronic low-grade and high-grade
366 synovitis. *Histopathology*. 2006; 49 (4): 358-64.
367 19. Pritzker K P, Gay S, Jimenez S A, Ostergaard K, Pelletier J P, Revell P A, et al.
368 Osteoarthritis cartilage histopathology: grading and staging. *Osteoarthritis Cartilage*.
369 2006; 14 (1): 13-29.
370 20. Inata Y, Piraino G, Hake P W, O'Connor M, Lahni P, Wolfe V, et al.
371 Age-dependent cardiac function during experimental sepsis: effect of pharmacological
372 activation of AMP-activated protein kinase by AICAR. *Am J Physiol Heart Circ*
373 *Physiol*. 2018; 315 (4): H826-h837.
374 21. Livshits G, Kalinkovich A. Hierarchical, imbalanced pro-inflammatory cytokine
375 networks govern the pathogenesis of chronic arthropathies. *Osteoarthritis Cartilage*.
376 2018; 26 (1): 7-17.
377 22. Siouti E, Andreakos E. The many facets of macrophages in rheumatoid arthritis.
378 *Biochem Pharmacol*. 2019; 165: 152-169.
379 23. Pascale V, Finelli R, Giannotti R, Coscioni E, Izzo R, Rozza F, et al. Cardiac
380 eccentric remodeling in patients with rheumatoid arthritis. *Sci Rep*. 2018; 8 (1): 5867.
381 24. Firestein G S, Corr M. Common mechanisms in immune-mediated inflammatory
382 disease. *J Rheumatol Suppl*. 2005; 73: 8-13; discussion 29-30.
383 25. Courtenay J S, Dallman M J, Dayan A D, Martin A, Mosedale B. Immunisation
384 against heterologous type II collagen induces arthritis in mice. *Nature*. 1980; 283

(5748): 666-8.

26. Matsuoka M, Onodera T, Sasazawa F, Momma D, Baba R, Hontani K, et al. An Articular Cartilage Repair Model in Common C57Bl/6 Mice. *Tissue Eng Part C Methods*. 2015; 21 (8): 767-72.

27. Nygaard G, Firestein G S. Restoring synovial homeostasis in rheumatoid arthritis by targeting fibroblast-like synoviocytes. *Nat Rev Rheumatol*. 2020; 16 (6): 316-333.

28. Burrage P S, Mix K S, Brinckerhoff C E. Matrix metalloproteinases: role in arthritis. *Front Biosci*. 2006; 11: 529-43.

29. Malemud C J. Matrix Metalloproteinases and Synovial Joint Pathology. *Prog Mol Biol Transl Sci*. 2017; 148: 305-325.

30. Liu W, Zhang Y, Zhu W, Ma C, Ruan J, Long H, et al. Sinomenine Inhibits the Progression of Rheumatoid Arthritis by Regulating the Secretion of Inflammatory Cytokines and Monocyte/Macrophage Subsets. *Front Immunol*. 2018; 9: 2228.

31. Uttra A M, Alamgeer, Shahzad M, Shabbir A, Jahan S. Ephedra gerardiana aqueous ethanolic extract and fractions attenuate Freund Complete Adjuvant induced arthritis in Sprague Dawley rats by downregulating PGE2, COX2, IL-1β, IL-6, TNF-α, NF-kB and upregulating IL-4 and IL-10. *J Ethnopharmacol*. 2018; 224: 482-496.

32. Udalova I A, Mantovani A, Feldmann M. Macrophage heterogeneity in the context of rheumatoid arthritis. *Nat Rev Rheumatol*. 2016; 12 (8): 472-85.

33. Shapiro S D, Kobayashi D K, Ley T J. Cloning and characterization of a unique elastolytic metalloproteinase produced by human alveolar macrophages. *J Biol Chem*. 1993; 268 (32): 23824-9.

34. Hu Y, Gui Z, Zhou Y, Xia L, Lin K, Xu Y. Quercetin alleviates rat osteoarthritis by inhibiting inflammation and apoptosis of chondrocytes, modulating synovial macrophages polarization to M2 macrophages. *Free Radic Biol Med*. 2019; 145: 146-160.

35. Kennedy A, Fearon U, Veale D J, Godson C. Macrophages in synovial inflammation. *Front Immunol*. 2011; 2: 52.

36. Van Raemdonck K, Umar S, Shahrara S. The pathogenic importance of CCL21 and CCR7 in rheumatoid arthritis. *Cytokine Growth Factor Rev*. 2020; 55: 86-93.

37. Van Raemdonck K, Umar S, Palasiewicz K, Volkov S, Volin M V, Arami S, et al. CCL21/CCR7 signaling in macrophages promotes joint inflammation and Th17-mediated osteoclast formation in rheumatoid arthritis. *Cell Mol Life Sci*. 2020; 77 (7): 1387-1399.

38. Moschovakis G L, Bubke A, Friedrichsen M, Ristenpart J, Back J W, Falk C S, et al. The chemokine receptor CCR7 is a promising target for rheumatoid arthritis therapy. *Cell Mol Immunol*. 2019; 16 (10): 791-799.

39. Smolen J S, Aletaha D, Koeller M, Weisman M H, Emery P. New therapies for treatment of rheumatoid arthritis. *Lancet*. 2007; 370 (9602): 1861-74.

40. Tu J, Hong W, Zhang P, Wang X, Körner H, Wei W. Ontology and Function of Fibroblast-Like and Macrophage-Like Synoviocytes: How Do They Talk to Each Other and Can They Be Targeted for Rheumatoid Arthritis Therapy? *Front Immunol*. 2018; 9: 1467.

41. Tu J, Wang X, Gong X, Hong W, Han D, Fang Y, et al. Synovial Macrophages in

Rheumatoid Arthritis: The Past, Present, and Future. *Mediators Inflamm*. 2020; 2020: 1583647.

42. Ota M, Tanaka Y, Nakagawa I, Jiang J J, Arima Y, Kamimura D, et al. Role of Chondrocytes in the Development of Rheumatoid Arthritis Via Transmembrane Protein 147-Mediated NF-κB Activation. *Arthritis Rheumatol*. 2020; 72 (6): 931-942.

43. Symmons D P, Gabriel S E. Epidemiology of CVD in rheumatic disease, with a focus on RA and SLE. *Nat Rev Rheumatol*. 2011; 7 (7): 399-408.

44. Lazúrová I, Tomáš Ľ. Cardiac Impairment in Rheumatoid Arthritis and Influence of Anti-TNFα Treatment. *Clin Rev Allergy Immunol*. 2017; 52 (3): 323-332.

45. Wang Z, Huang W, Ren F, Luo L, Zhou J, Huang D, et al. Characteristics of Ang-(1-7)/Mas-Mediated Amelioration of Joint Inflammation and Cardiac Complications in Mice With Collagen-Induced Arthritis. *Front Immunol*. 2021; 12: 655614.

46. Giles J T, Fernandes V, Lima J A, Bathon J M. Myocardial dysfunction in rheumatoid arthritis: epidemiology and pathogenesis. *Arthritis Res Ther*. 2005; 7 (5): 195-207.

447 **Table 1. Sequences of primers utilized in this study**

Name	Sequence	Product length (bp)
AKAP12 Fwd	TGGGAGGCGTTGATTTG	169
AKAP12 Rv	GGTCTTGTTCCTGGGTGC	
IL-6 Fwd	ATGGCAATTCTGATTGTATG	212
IL-6 Rv	GACTCTGGCTTTGTCTTTCT	
TNF-α Fwd	CAGGCGGTGCCTATGTCTCA	182
TNF-α Rv	GCTCCTCCACTTGGTGGTTT	
iNOS Fwd	CACCACCCTCCTCGTTC	132
iNOS Rv	CAATCCACAACTCGCTCC	
IL-10 Fwd	TTAAGGGTTACTTGGGTTGC	137
IL-10 Rv	GAGGGTCTTCAGCTTCTCAC	
Arginase-1 Fwd	TATCTGCCAAAGACATCG	130
Arginase-1 Rv	ATCACCTTGCCAATCCC	

448 Note: Fwd, Forward; Rv, Reverse

449

Figures and figure legend

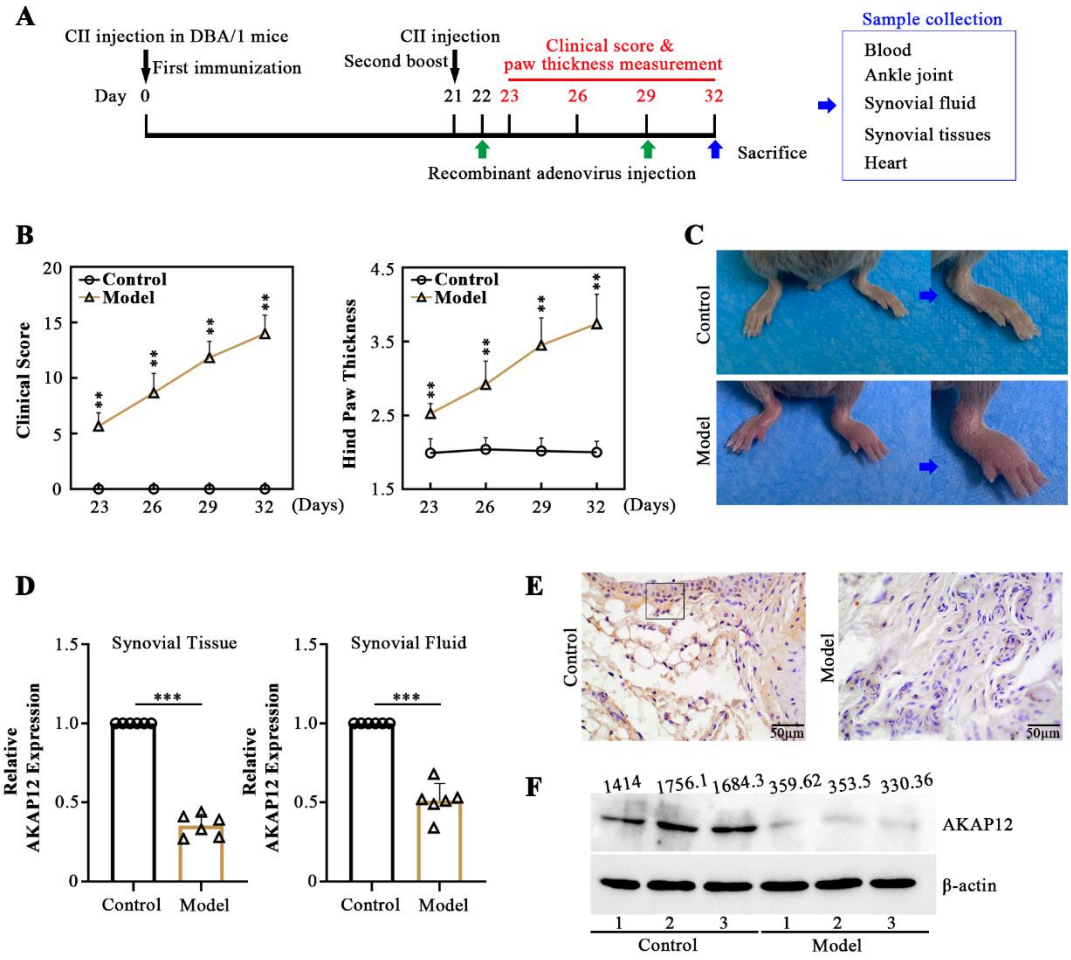

Figure 1 AKAP12 level is decreased in a CIA mouse model. Analysis of RA progression was based on a collagen-induced arthritis (CIA) mouse model. (A) Experimental procedure was shown. (B) The clinical scores were recorded and paw thickness was measured every 3 days beginning 23 days after the initial immunization. (C) Photographs of hind paws 32 days after modeling. (D) AKAP12 mRNA expression in synovial tissues and fluid was determined by quantitative PCR. (E) Immunohistochemical staining of AKAP12 in synovial tissues. (F) Representative band images of AKAP12 via western blot. Data are shown as mean ± standard deviation (SD), *p*-values: ** <0.01, *** <0.001.

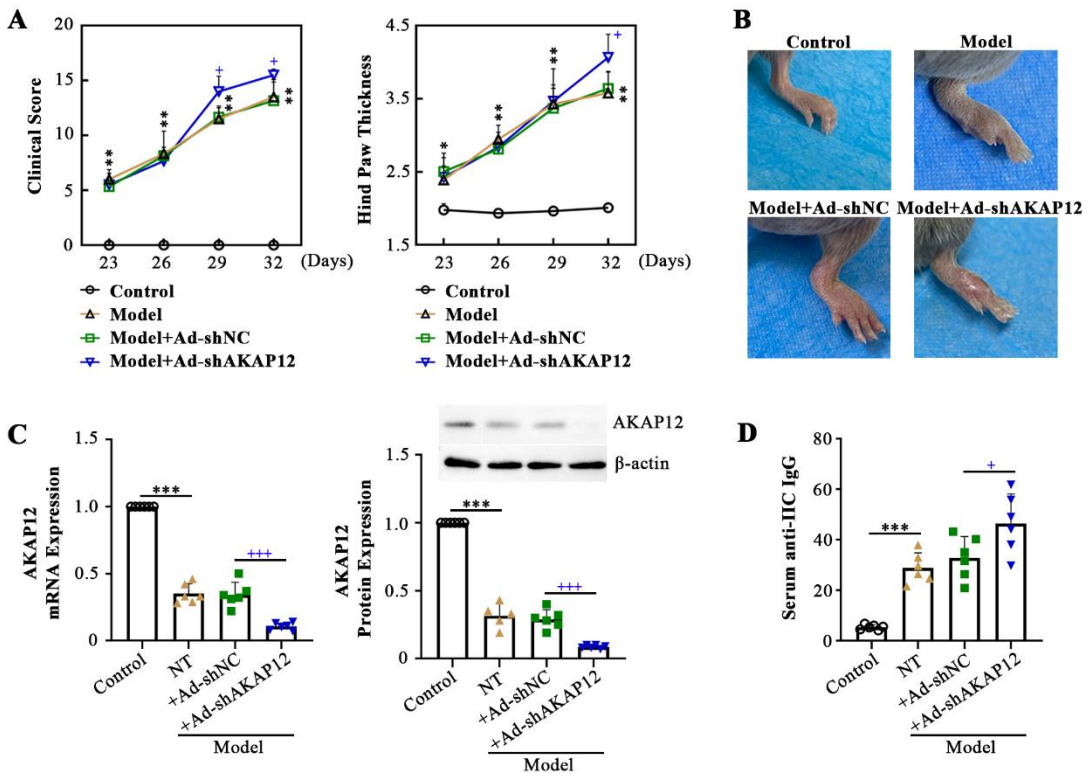

Figure 2 Loss of AKAP12 worsens CIA progression. One day after booster immunization, the mice received Ad-shAKAP12 or Ad-shNC (once per week) via tail vein injection. (A) Clinical assessment and paw thickness measurement on day 23, 26, 29 and 32. (B) Pictures of hind paws on day 32 were displayed. (C) Quantitative PCR and western blot analysis of AKAP12 expression in synovial tissues. (D) Detection of serum anti-IIC antibody level by ELISA. NT, not treated. Data are shown as mean ± standard deviation (SD), *p*-values: * <0.05, ** <0.01, *** <0.001; + <0.05, +++ <0.001.

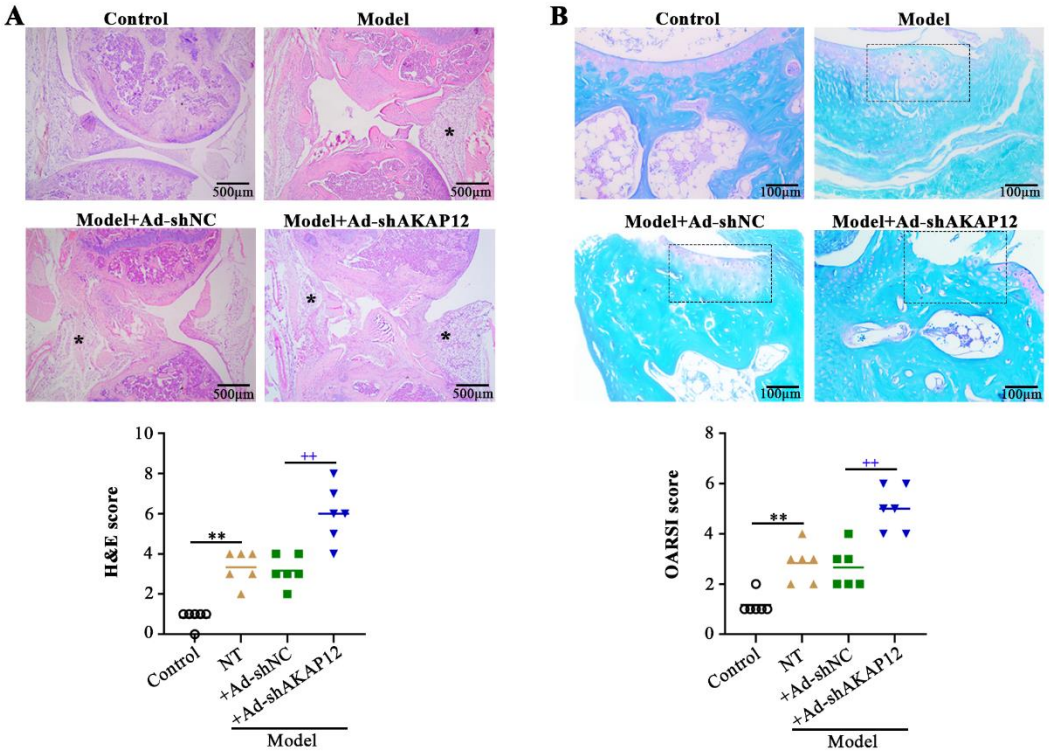

Figure 3 Histopathological analysis of tissues. (A) Pathological observation of synovial tissues (H&E staining) and subsequent scoring. * indicates inflammatory infiltration of synovium. (B) Evaluation of cartilage damage (box) in ankle joints by Safranin *O*-fast green staining, and OARSI scoring. NT, not treated. Data are indicated as mean ± standard deviation (SD), *p*-values: ** <0.01; ++ <0.01.

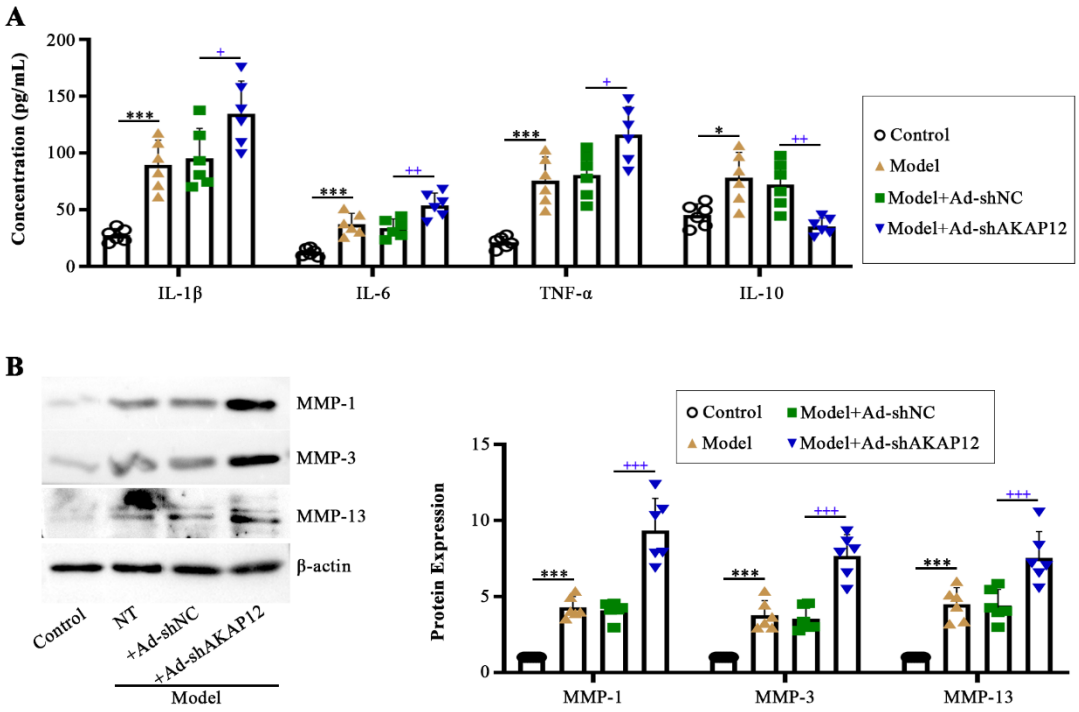

476

477 **Figure 4 Loss of AKAP12 affects the production of inflammatory cytokines and**

478 **MMPs in CIA mice.** (A) Serum levels of IL-1β, IL-6, TNF-α and IL-10 were

479 detected by ELISA. (B) Western blot analysis of MMP-1, MMP-3 and MMP-13 in

480 synovial tissues. NT, not treated. Data are shown as mean ± standard deviation (SD),

481 *p*-values: * <0.05, *** <0.001; + <0.05, ++ <0.01, +++ <0.001.

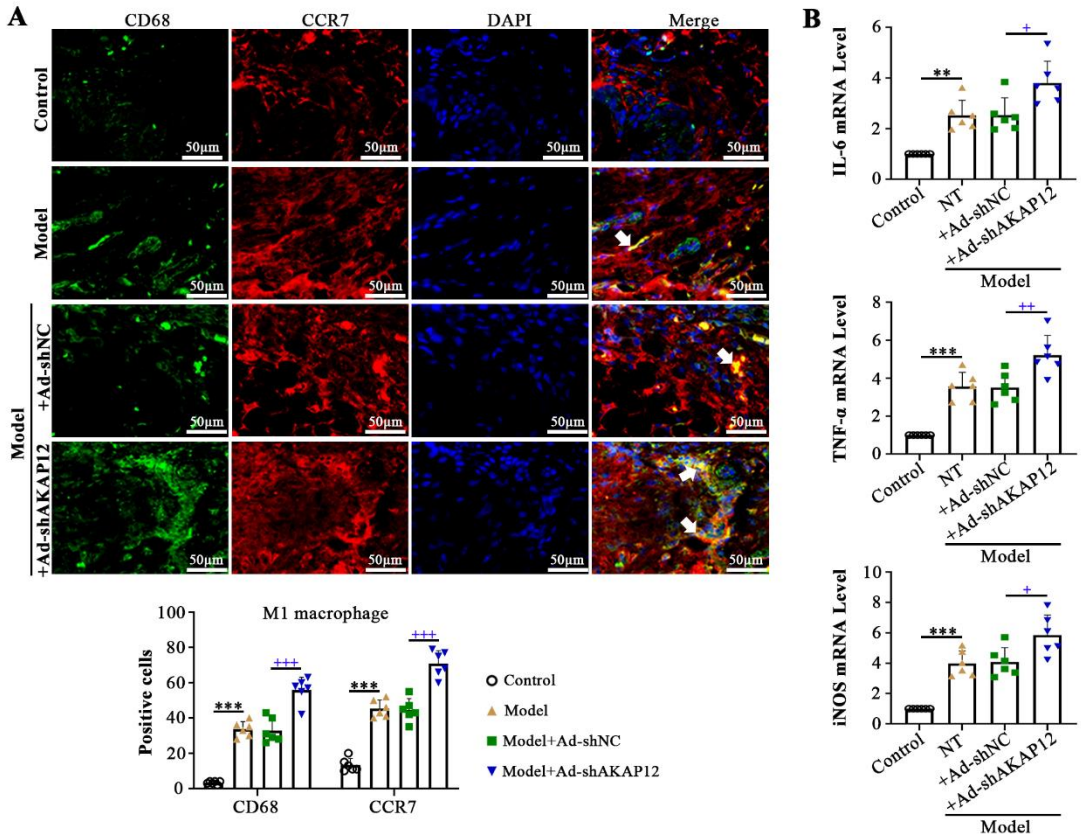

482

483 **Figure 5 Loss of AKAP12 modulates M1 macrophage polarization in CIA mice.**

484 (A) Representative images of immunofluoresence double staining of CD68 (green)

485 and CCR7 (red), and quantification of the number of $CD68^+$ macrophages and $CCR7^+$

486 M1 macrophages. (B) Quantitative PCR was utilized for mRNA expression levels of

487 IL-6, TNF-α and iNOS, three markers of M1 macrophages. Data are represented as

488 mean ± standard deviation (SD), *p*-values: * <0.05, ** <0.01, *** <0.001; + <0.05,

489 ++ <0.01, +++ <0.001.

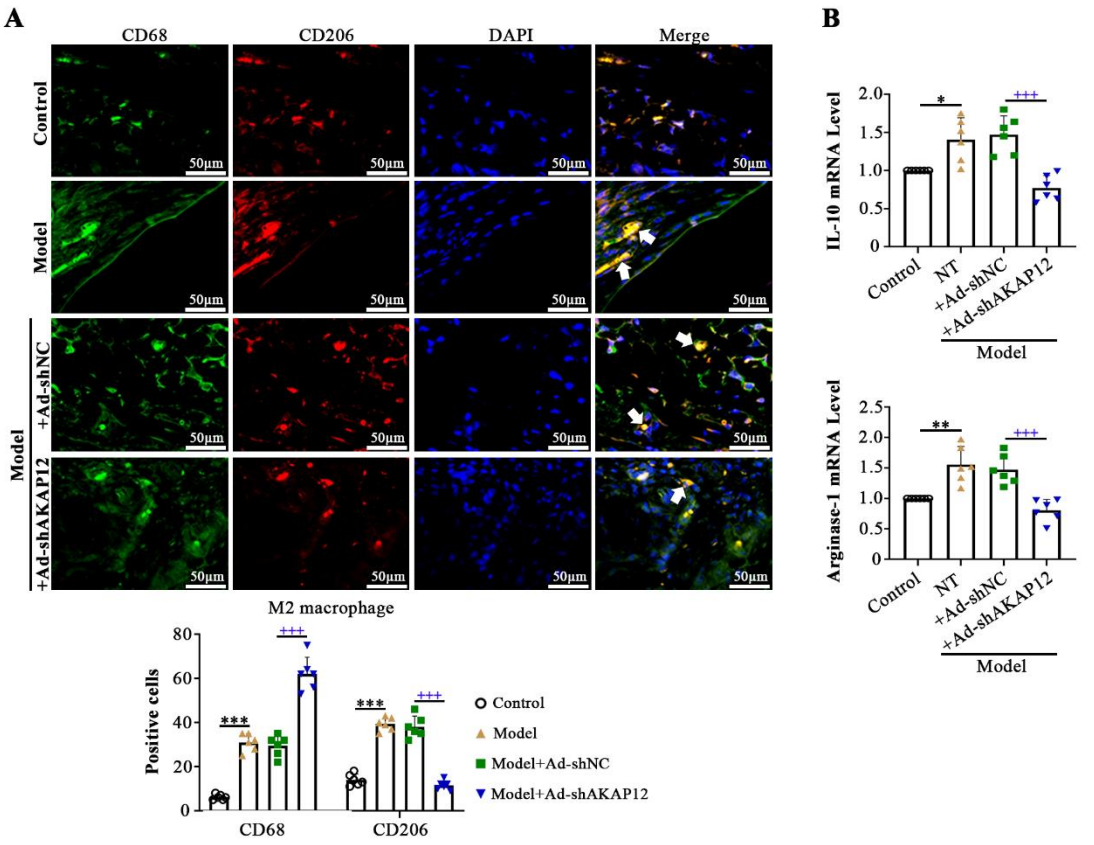

490

491 **Figure 6 Loss of AKAP12 inhibits M2 macrophage polarization.** (A)

492 Immunofluoresence double staining of CD68 (green) and CD206 (red), followed by

493 quantification of $CD68^{+}/CCR7^{+}$ macrophages. (B) Detection of M2 macrophage

494 markers (IL-10 and arginase-1) using quantitative PCR. Data are represented as mean

495 ± standard deviation (SD), *p*-values: * <0.05, ** <0.01, *** <0.001; + <0.05, ++

496 <0.01, +++ <0.001.

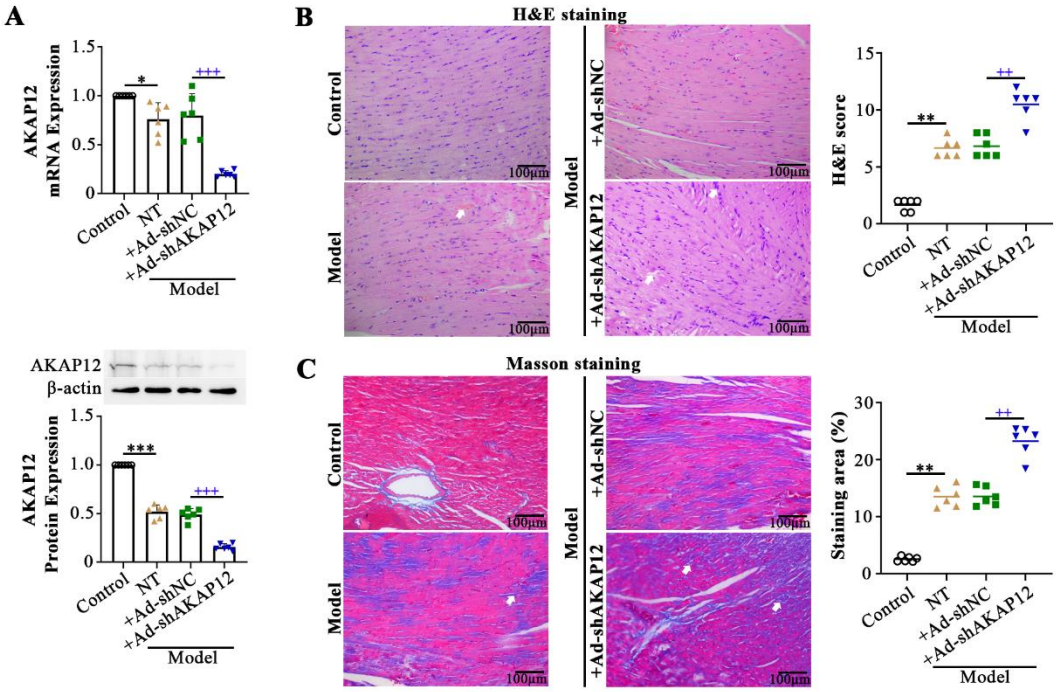

Figure 7 Loss of AKAP12 worsens cardiac damage of CIA mice. (A) Quantitative PCR and western blot assays were performed to measure AKAP12 expression level in hearts. (B, C) Representative photographs showed H&E and Masson's trichrome staining of heart tissues, and assessment of heart damage and fibrosis (scoring). NT, not treated. Data are represented as mean ± standard deviation (SD), *p*-values: * <0.05, ** <0.01, *** <0.001; ++ <0.01, +++ <0.001.